J Pharmacokinet Pharmacodyn (2011) 38:743–767
DOI 10.1007/s10928-011-9218-0

The influence of distributional kinetics into a peripheral compartment on the pharmacokinetics of substrate partitioning between blood and brain tissue

Jeannie M. Padowski · Gary M. Pollack

Received: 18 May 2011 / Accepted: 21 September 2011 / Published online: 9 October 2011

Abstract Development of CNS-targeted agents often focuses on identifying compounds with "good" CNS exposure (brain-to-blood partitioning >1). Some compounds undergoing enterohepatic recycling (ER) evidence a partition coefficient, $K_{p,brain}$ (expressed as C_{brain}/C_{plasma}), that exceeds and then decreases to (i.e., overshoots) a plateau (distribution equilibrium) value, rather than increasing monotonically to this value. This study tested the hypothesis that overshoot in $K_{p,brain}$ is due to substrate residence in a peripheral compartment. Simulations were based on a 3-compartment model with distributional clearances between central and brain (CL_{br}) and central and peripheral (CL_d) compartments and irreversible clearance from the central compartment (CL). Parameters were varied to investigate the relationship between overshoot and peripheral compartment volume (V_p), and how this relationship was modulated by other model parameters. Overshoot magnitude and duration were characterized as peak C_{brain}/C_{plasma} relative to the plateau value ($\%OS$) and time to reach plateau (TRP). Except for systems with high CL_d, increasing V_p increased TRP and $\%OS$. Increasing brain (V_{br}) or central (V_c) distribution volumes eliminated V_p-related OS. Parallel increases in all clearances

J. M. Padowski · G. M. Pollack
Curriculum in Toxicology, School of Medicine and Division of Pharmacotherapy and Experimental Therapeutics, School of Pharmacy, University of North Carolina at Chapel Hill, Chapel Hill, NC, USA

Present Address:
J. M. Padowski
Department of Radiology, University of Washington, Box 357115, 1959 NE Pacific Street, AA-010A, Seattle, WA 98195, USA
e-mail: padowski@u.washington.edu

G. M. Pollack (✉)
College of Pharmacy, Washington State University, 105F Wegner Hall, PO Box 646510, Pullman, WA 99164, USA
e-mail: gary.pollack@wsu.edu

shortened *TRP*, but did not alter *%OS*. Increasing either *CL* or CL_d individually increased *%OS* related to V_p, while increasing CL_{br} decreased *%OS*. Under realistic peripheral distribution scenarios, C_{brain}/C_{plasma} may overshoot substantially $K_{p,brain}$ at distribution equilibrium. This observation suggests potential for erroneous assessment of brain disposition, particularly for compounds which exhibit a large apparent V_p, and emphasizes the need for complete understanding of distributional kinetics when evaluating brain uptake.

Keywords Blood–brain barrier · Tissue partitioning · Distributional kinetics · Central nervous system · Enterohepatic recycling · Valproic acid

Introduction

Therapeutic agents cannot be effective unless they reach their sites of action within the body at a sufficient rate and extent to produce the desired pharmacologic effect. Relatively few effective pharmaceuticals exist for brain and central nervous system (CNS) disorders; the majority of CNS diseases are essentially refractory to small-molecule drug therapy, despite a relative large "neurotherapeutic space" (i.e., the number of relevant receptor targets for brain disorders) [1]. The lack of effective CNS therapeutics across the broad range of neurologic diseases is due, in large part, to the existence of a network of specialized physical and biochemical features at the interface between the systemic circulation and the brain parenchyma [2], collectively termed the blood–brain barrier (BBB), which tightly regulates the passage of xenobiotics between these two environments [3, 4]. Often this minimal penetration to the brain parenchymal space is a useful characteristic, as it limits CNS toxicity associated with agents developed to treat non-CNS diseases. For CNS drug development, however, a major goal is identification of compounds which are capable of penetrating the BBB to achieve sufficient brain exposure [5]. In fact, the most significant limitation in the development of new therapeutic agents to treat CNS disorders is the ability to distribute across the blood–brain barrier [6].

The relationships among drug physicochemical properties, brain exposure, and pharmacologic efficacy are complicated. Factors which influence the rate and extent of drug exposure in the brain include passive membrane permeability, protein binding, ionization, metabolism at the blood–brain interface, active uptake and efflux at the BBB, and CSF bulk flow [7]. Factors which influence the relationship between exposure and efficacy obviously add another level of complexity to the most important relationship: that between the properties of a drug and its ability to elicit the desired pharmacologic response.

A thorough investigation of the interacting factors that dictate brain exposure is not feasible when screening the pharmacokinetic and pharmacodynamic properties of large numbers of compounds. The pharmaceutical industry has therefore based its lead optimization strategy for CNS compounds largely upon measurement of the ratio of substrate partitioning between brain tissue and blood [8, 9]. Drugs with partition ratios exceeding unity are somewhat arbitrarily considered to have "good" CNS penetration.

This ratio, termed the brain-to-blood partition coefficient, $K_{p,brain}$, can be calculated as the ratio of the area under the concentration–time curves (AUC) in brain vs. plasma (AUC_{brain}/AUC_{plasma}), thereby providing a time-independent estimate of relative tissue exposure. More practically, $K_{p,brain}$ often is expressed as the ratio of concentrations in brain vs. blood (C_{brain}/C_{plasma}) at a discrete point in time during or following drug administration. This expression of partitioning is, of course, inherently time-dependent, and may be symbolized most appropriately as $K^{t}_{p,brain}$. Under the special condition of distributional equilibrium or system steady-state, partitioning may be symbolized as $K^{DE}_{p,brain}$ or $K^{SS}_{p,brain}$. For simplicity, we will use the term $K_{p,brain}$ to indicate partitioning under conditions of distribution equilibrium.

Regardless of the particular method used to express partitioning, the utility of this metric as a predictor of potential CNS activity has been debated [10]. It arguably is somewhat simplistic, and in reality compounds that exhibit therapeutic efficacy in brain may have $K_{p,brain}$ values substantially lower than unity [11]. Nevertheless, $K_{p,brain}$ remains common as a fairly straightforward and useful general metric of brain exposure [12], and so it is necessary to understand the various factors that impact the predictive quality of this metric.

One important factor that can complicate the use of partition coefficients to assess brain exposure is the time-dependency inherent in this measurement. As the entire mass of substrate initially exists in the systemic circulation immediately following intravenous or intra-arterial administration, the ratio of substrate concentration in brain vs. blood increases from zero with time as the substrate equilibrates between these two compartments [13]. The point in time at which substrate concentrations in brain and blood begin to change in parallel is referred to as brain-to-blood distribution equilibrium. The degree of brain partitioning at distribution equilibrium represents the partitioning under physiologically- and pharmacologically-relevant conditions (i.e., repeated administration). Therefore, $K_{p,brain}$ is appropriately calculated from brain-to-blood concentration ratios when those concentrations are measured either at distribution equilibrium or at system-wide steady-state, which can only be achieved after distribution equilibrium has been attained. This metric also can be based upon unbound, rather than total, drug concentration, allowing evaluation of the substrate distribution across the blood–brain barrier in the absence of impedance due to protein binding in blood. This approach can support a mechanistic elaboration of distributional processes across the blood–brain interface, although tissue exposure (relative to systemic exposure) typically is based upon total substrate concentration.

Although very little discussion exists in the literature, it generally is assumed that the partition coefficient increases monotonically from time zero through the attainment of distribution equilibrium. A simulation study, which evaluated the relationship between sampling time prior to distribution equilibrium and the observed C_{brain}/C_{plasma} ratio in the presence vs. absence of BBB efflux transport, indicated that in some cases C_{brain}/C_{plasma} rose to an initial peak value, then decreased to a value which remained constant with time [14]. This overshoot of the plateau ($K_{p,brain}$) value occurred when the distribution behavior of hypothetical

compounds was simulated with a relatively large peripheral (non-brain) volume of distribution.

This type of overshoot behavior has been observed for some compounds. One relevant example is the branched-chain fatty acid anticonvulsant, valproic acid (VPA) [15–18]. VPA undergoes enterohepatic recycling, which confers unique peripheral distribution kinetics [19–21]. Because the majority of VPA entering this enterohepatic loop eventually returns to the systemic circulation as parent drug, recycling essentially functions as a peripheral pharmacokinetic compartment with a large apparent volume of distribution [21].

The accuracy with which $K_{p,brain}$ expresses the true brain-to-blood partitioning of a substrate depends upon identification of the plateau C_{brain}/C_{plasma} ratio. Thus, the existence of a region of overshoot in the C_{brain}/C_{plasma} vs. time profile could complicate assessment of brain partitioning, particularly if the peak partition ratio is assumed to represent the ratio which would be observed at distribution equilibrium ($K_{p,brain}$). Moreover, the existence of this currently-unexplained partition coefficient overshoot reveals that there are fundamental aspects of brain-to-blood partitioning kinetics which have not been appreciated.

Based upon the relationship observed in previous simulations [14] between overshoot in the C_{brain}/C_{plasma} vs. time profile and the apparent volume of a functional peripheral compartment, the present simulation study was undertaken to investigate the influence of distribution into a peripheral pharmacokinetic compartment on the C_{brain}/C_{plasma} vs. time profile. Secondary objectives of this study were to develop mathematical descriptors of the shape of the C_{brain}/C_{plasma} vs. time profile and to elucidate the relationship between these descriptors and relevant pharmacokinetic parameters in a simple simulated system. Finally, examples of brain partitioning for compounds undergoing various extents of enterohepatic recycling were mined from the literature in order to demonstrate the relevance of large apparent peripheral volumes to the overshoot in equilibrium brain partitioning under actual experimental conditions.

Materials and methods

Definitions

To evaluate the effect of peripheral (non-brain) compartment distribution kinetics on the C_{brain}/C_{plasma} vs. time profile, it was necessary to establish terminology to describe the shape of this profile (Fig. 1). C_{brain}/C_{plasma} ratios calculated under pharmacologically-relevant conditions (i.e., at brain-to-blood distribution equilibrium) are generally termed $K_{p,brain}$. For the purposes of this study, $K_{p,brain}$ refers to the "plateau" C_{brain}/C_{plasma} value, defined as the C_{brain}/C_{plasma} ratio that remained constant through the end of the simulated time domain (until numerical solutions to the model became unstable as substrate mass in the system approached zero). Overshoot (OS) was defined as a C_{brain}/C_{plasma} ratio that exceeded plateau by >10% (in practical terms, a degree of precision below which the measured value would be indistinguishable from the eventual plateau value). Overshoot for each simulation

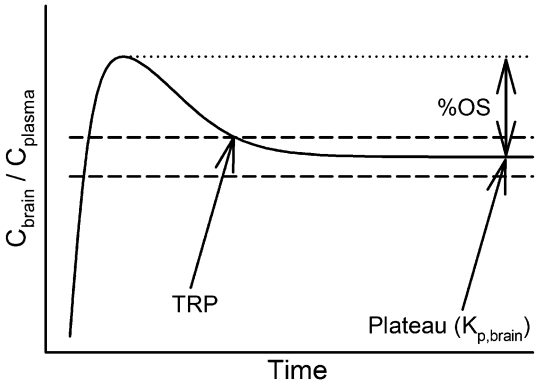

Fig. 1 Schematic of the time course of substrate partitioning between brain tissue and blood demonstrating the overshoot phenomenon. *Dashed lines* represent the presumed uncertainty around the brain-to-plasma concentration ratio at distribution equilibrium ($K_{p,brain}$). *TRP* represents the time at which the concentration ratio would have been considered to have returned to the plateau value under realistic experimental conditions. The difference between the highest value of the concentration ratio in the profile relative to the plateau value was defined as percent overshoot (*%OS*)

was quantified in terms of magnitude (peak C_{brain}/C_{plasma} ratio expressed as a percentage of the plateau value; *%OS*) and duration. Duration of overshoot (as time of return to plateau; *TRP*) was defined as the first time point at which the C_{brain}/C_{plasma} value fell to within 10% of the plateau value.

Pharmacokinetic models

Figure 2 illustrates the structure of the pharmacokinetic model utilized in this simulation study. This 3-compartment model, representing brain, plasma, and a peripheral compartment, was constructed as the simplest system in which to evaluate the influence of distribution into a peripheral pharmacokinetic compartment on substrate partitioning between brain and plasma. Distributional clearances between the systemic circulation (plasma) and brain (CL_{br}), and between plasma and the peripheral compartment (CL_d), were assumed to be bidirectional, first-order processes. Systemic clearance (CL), mediated from the central compartment, was assumed to be unidirectional and first-order. For simplicity, protein binding was ignored. Input was modeled as a single i.v. bolus dose at $t = 0$. The relevant differential equations are

$$\frac{dC_{brain}}{dt} = (C_{plasma} \cdot CL_{br} - C_{brain} \cdot CL_{br})/V_{br} \quad (1)$$

$$\frac{dC_{peripheral}}{dt} = (C_{plasma} \cdot CL_{d} - C_{peripheral} \cdot CL_{d})/V_{p} \quad (2)$$

$$\frac{dC_{plasma}}{dt} = (C_{peripheral} \cdot CL_{d} + C_{brain} \cdot CL_{br} - C_{plasma} \cdot (CL_{d} + CL_{br} + CL))/V_{c} \quad (3)$$

where C_{brain}, $C_{peripheral}$, and C_{plasma} represent concentrations in brain tissue, the peripheral pharmacokinetic compartment, and the central compartment, and V_{br}, V_p,

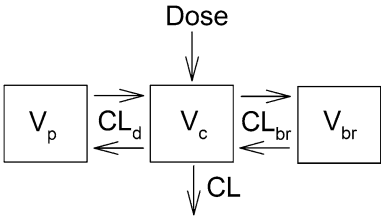

Fig. 2 Structure of the 3-compartment model used for simulation studies. See text for definition of model parameters

and V_c represent the apparent volumes of the brain, peripheral, and central compartments.

In order to characterize fundamental aspects of system behavior, relationships between the various descriptive indices (e.g., *%OS*, *TRP*) of the brain partitioning vs. time profile and model parameters (e.g., V_p) were evaluated with empirical models (structurally analogous to E_{max} or sigmoidal E_{max} models, as presented below)

$$E = \frac{(E_{max} \cdot V_p)}{V_p + V_{p,50}} \tag{4}$$

$$E = \frac{(E_{max} \cdot V_p^{\gamma})}{(V_p^{\gamma} + V_{p,50}^{\gamma})} \tag{5}$$

where E represents the descriptive parameter under consideration (*%OS* or *TRP*), E_{max} represents the highest value achievable as V_p approaches infinity, $V_{p,50}$ is the volume of the peripheral compartment associated with half-maximal *%OS* or *TRP*, and γ is a shape factor.

All simulation and modeling was conducted using WinNonlin 5.0.1 (Pharsight, Mountain View, CA).

Parameter selection

A default parameter space $\{P\}_D$ was established as both a starting point for initiation of simulation experiments and as a template against which to compare the effects of parameter manipulation. This parameter space consisted of the three clearance terms (Fig. 2), each set at 2.5 ml/min/kg, brain and plasma volumes fixed at values consistent with rat physiology (15 and 50 ml/kg), and a peripheral distribution volume (V_p) of zero. These parameter values were selected such that manipulation of the V_p term upward from zero would elicit the appearance of a range of overshoot behavior in the associated C_{brain}/C_{plasma} vs. time profiles. For the purposes of this simulation study, V_p values were varied from zero through 50 l/kg.

Three different parameter spaces (created by manipulating the V_p term within $\{P\}_D$) were selected to produce C_{brain}/C_{plasma} vs. time profiles representative of low, intermediate, or high degrees of overshoot. These three representative parameter spaces, termed $\{P\}_1$, $\{P\}_2$, and $\{P\}_3$, were used as reference points for evaluation of the effect of manipulating various parameters (other than V_p) on overshoot behavior in systems in which the degree of V_p-related overshoot was initially low,

intermediate, or high. The effects of each parameter on the shape (*%OS*, *TRP*) of the C_{brain}/C_{plasma} vs. time profile were investigated independently or in parallel by perturbing each parameter value relative to its default $\{P\}_D$ value. Brain and plasma volumes were varied up to 50-fold relative to the default values. Perturbation of clearance values was constrained to an upper limit of 25 ml/min/kg.

Results

Peripheral compartment volume

In order to evaluate the influence of substrate distribution into a peripheral compartment on the shape of the C_{brain}/C_{plasma} vs. time profile, an initial simulation experiment was conducted with the goals of exploring the range of system responses and informing the design of subsequent simulation studies. Beginning with the default parameter space ($\{P\}_D$) where V_p was zero, the disposition of several different hypothetical compounds was simulated by manipulating the V_p parameter alone. The resulting C_{brain}/C_{plasma} vs. time relationships are illustrated in Fig. 3a.

Several trends were identified in association with the changes in the apparent volume of the peripheral compartment. First, plateau values ($K_{p,brain}$) clearly were influenced by V_p, although to a somewhat modest extent (<33% relative change). As V_p increased from 2 to 20 ml/kg, the plateau C_{brain}/C_{plasma} value decreased from 1.3 to 1.2. Further increases in V_p elicited progressively smaller decrements in the plateau C_{brain}/C_{plasma} value, to a minimum of 0.95 at the largest peripheral compartment volume evaluated. Second, although the rate of the initial rapid increase in C_{brain}/C_{plasma} immediately post-dose appeared similar for all simulation scenarios, when V_p exceeded 20 ml/kg this early increase in C_{brain}/C_{plasma} persisted longer, and C_{brain}/C_{plasma} evidenced overshoot relative to the eventual plateau value. As V_p increased from 0.1 to 50 l/kg, the maximum observed value of C_{brain}/C_{plasma} increased in both absolute and relative (to plateau value) terms, peaking at a C_{brain}/C_{plasma} ratio of 1.7 (64%*OS*).

The relationship between overshoot magnitude and V_p is depicted in Fig. 3b. An empirical sigmoidal model (Eq. 5) was fit to these data in order to identify the fundamental parameters that are descriptive of this relationship (Table 1). The model fit to the data generated an estimate of a theoretical maximum possible *%OS* value of 64% that could be achieved by increasing V_p within $\{P\}_D$. The V_p associated with a half-maximal overshoot ($V_{p,50}$) was 131 ml/kg. The gamma value, describing the steepness of the sigmoidal relationship, was 1.24. The coefficients of variation for parameter estimates recovered through this analysis were below 10% for each parameter in the model.

V_p was the parameter of primary interest in these simulations. Therefore, the *%OS* vs. V_p profile (Fig. 3b) resulting from manipulation of V_p within $\{P\}_D$ served as a baseline against which to evaluate the effects of manipulating other (non-V_p) system parameters. Essentially, to determine how non-V_p parameters might interact with V_p to affect the C_{brain}/C_{plasma} vs. time profile, it was necessary to establish "reference" parameter spaces in which, for example, both V_p and overshoot were

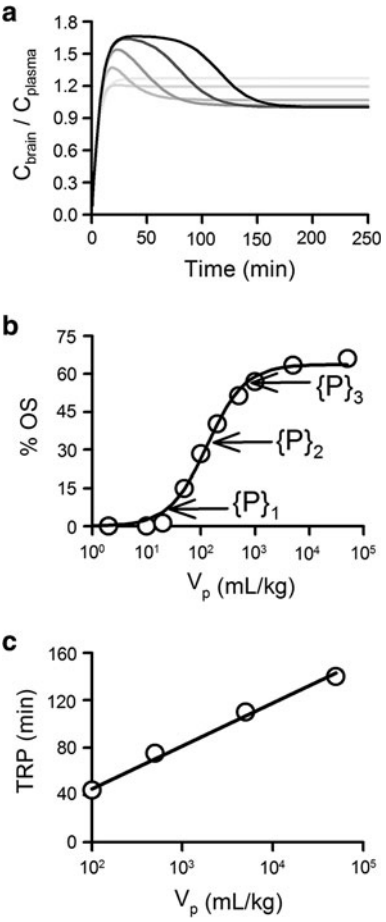

Fig. 3 Influence of V_p on the kinetics of substrate partitioning into brain (**a**). Default parameter values were used, and V_p was increased from 2 ml/kg to 50 l/kg (profiles progressing from light to dark). A sigmoidal model (Eq. 5) was capable of describing the relationship between *%OS* and V_p resulting from these simulations (**b**). The time required for the brain-to-plasma concentration ratio to return to the plateau value, as illustrated in Fig. 1, was a log-linear function of V_p (**c**). *Arrows* indicate the *%OS* vs. V_p relationship of three parameter spaces selected for use in subsequent simulations ($\{P\}_1$, $\{P\}_2$ and $\{P\}_3$)

Table 1 Results of fitting a sigmoidal E_{max} model to *%OS* vs. V_p data from Fig. 3b

	E_{max} (%)	$V_{p,50}$ (ml/kg)	γ
Estimate	63.7	131	1.24
Standard error	1.68	11.3	0.124
CV%	2.64	8.60	9.95

"low", or in which V_p and overshoot were "high", when all other parameters were identical between the systems. Based upon the fit of the sigmoidal model (solid line) to the *%OS* vs. V_p profile illustrated in Fig. 3b, three such "reference" parameter spaces ($\{P\}_1$, $\{P\}_2$ and $\{P\}_3$) were created as examples of conditions of "low", "intermediate" or "high" V_p-related overshoot. These parameter spaces were generated by adjusting V_p within $\{P\}_D$ to create C_{brain}/C_{plasma} vs. time profiles with *%OS* values that were 10%, 50%, or 90% of the maximum predicted *%OS* achievable by adjusting V_p within the default parameter space (Fig. 3b). Since the maximum *%OS* achievable by adjusting V_p within $\{P\}_D$ was 64%, the *%OS* values

associated with $\{P\}_1$, $\{P\}_2$ and $\{P\}_3$ were 6.4%, 32%, and 58%. V_p for $\{P\}_1$, $\{P\}_2$ and $\{P\}_3$ was set at 23.4, 140 and 833 ml/kg. All other parameters values were identical between these three systems and $\{P\}_D$. These three parameter spaces were used in subsequent simulation studies as starting points for examination of the effect of manipulating parameters other than V_p on overshoot behavior in systems for which the degree of V_p-related overshoot was initially low, intermediate, or high.

Increasing V_p extended the amount of time required to achieve the final plateau C_{brain}/C_{plasma} value (Fig. 3a). For scenarios in which V_p was smaller than 100 ml/kg, the plateau C_{brain}/C_{plasma} value was attained earliest, as no overshoot was present. Although scenarios incorporating larger V_p values had slightly lower plateau C_{brain}/C_{plasma} ratios, the time at which C_{brain}/C_{plasma} returned to within 10% of its plateau value (*TRP*) increased in a log-linear manner with increases in V_p (Fig. 3c). As scenarios with the lowest V_p values evidenced no functionally-defined overshoot (<10%*OS*), only four different simulation scenarios are represented in Fig. 3c. The C_{brain}/C_{plasma} ratio associated with the largest V_p (50 l/kg) did not decrease to within 10% of its plateau value until approximately 160 min; in contrast, return to 10% of the eventual plateau value occurred within 45 min when V_p was 100 ml/kg.

Relative mass in each compartment

To examine how V_p influences the disposition of substrate in brain and plasma, the time course of substrate disposition in each compartment was evaluated under conditions of both small and large V_p, producing low and high degrees of overshoot. The two representative parameter spaces were selected (by altering V_p within $\{P\}_D$, as described above) to produce C_{brain}/C_{plasma} vs. time profiles with %*OS* values that were 10% and 90% of the maximum %*OS* achievable within $\{P\}_D$ ($\{P\}_1$ and $\{P\}_3$; Fig. 3b). For $\{P\}_1$ (Fig. 4a) and $\{P\}_3$ (Fig. 4b), the substrate mass in each compartment was plotted vs. time. Based upon visual comparison, it is apparent that manipulation of V_p alters the time course of substrate disposition in all three compartments, as opposed to only within the peripheral and central compartments.

Within the small V_p ($\{P\}_1$; Fig. 4a) parameter space, the substrate mass in the brain and peripheral compartments peaked relatively early (approximately 20 min), with the mass in the peripheral compartment remaining lower than that in plasma, but higher than that in brain. Mass in all three compartments began to decline at a fixed ratio (indicating attainment of distribution equilibrium) by approximately 30 min, and decreased at a consistent rate in each compartment throughout the remainder of the time domain.

Within the large V_p ($\{P\}_3$; Fig. 4b) parameter space, a larger fraction of the mass in the system accumulated in the peripheral compartment, where it was almost completely retained over the relevant time domain. Accordingly, mass in the brain and plasma compartments declined at a higher initial rate, with the rate of loss from plasma exceeding the rate of loss from brain (i.e., producing overshoot in the ratio of C_{brain}/C_{plasma}). At approximately 60 min, a decrease in the rate of loss of substrate from brain and plasma was observed, and the system attained distribution equilibrium by approximately 125 min. At these late time points, mass in all three

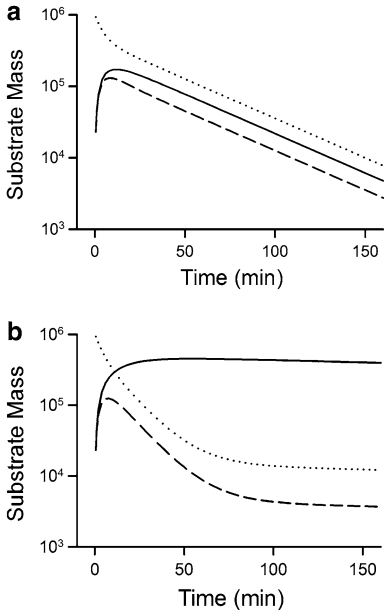

Fig. 4 Influence of V_p on the time course of substrate disposition (*dotted*, *dashed* and *solid lines* indicate central, brain tissue and peripheral compartments). Representative simulated mass vs. time relationships are displayed for parameter spaces $\{P\}_1$ (**a**) and $\{P\}_3$ (**b**) illustrating low and high V_p-related overshoot

compartments was declining more slowly, relative to conditions observed within $\{P\}_1$ in which V_p was low.

Influence of absolute clearances

As the previous experiments demonstrated a clear influence of V_p on overshoot behavior within $\{P\}_D$, the following simulation studies were conducted to determine whether the effects of V_p could be modified by manipulation of the clearance terms. The first of these simulations evaluated the effect of changing the absolute values of the three clearance terms by perturbing CL, CL_d and CL_{br} in parallel (to retain the relative relationship between the terms) 10-fold upward and 10-fold downward from the $\{P\}_D$ values of 2.5 ml/min/kg.

Beginning with $\{P\}_D$, six different parameter spaces were established by incorporating V_p ranging from 2 ml/kg to 50 l/kg. Within each parameter space, C_{brain}/C_{plasma} vs. time profiles were simulated, and $\%OS$ and TRP were determined and plotted vs. V_p (Fig. 5a, b; gray symbols). As scenarios incorporating the lowest V_p evidenced no functional overshoot, only four simulation conditions are illustrated in Fig. 5b. Subsequently, all three clearance values were simultaneously (maintaining their 1:1:1 ratio) either decreased to 0.25 ml/min/kg or increased to 25 ml/min/kg within each of the six parameter spaces. The effects of decreased (open symbols) or increased (black symbols) absolute clearance values on the V_p vs. $\%OS$ and V_p vs. TRP relationships are illustrated in Fig. 5.

The sigmoidal relationship between $\%OS$ and V_p remained static regardless of the absolute clearance values (Fig. 5a; open, gray and black symbols completely overlap). The relationship between TRP and V_p remained log-linear, with increasing

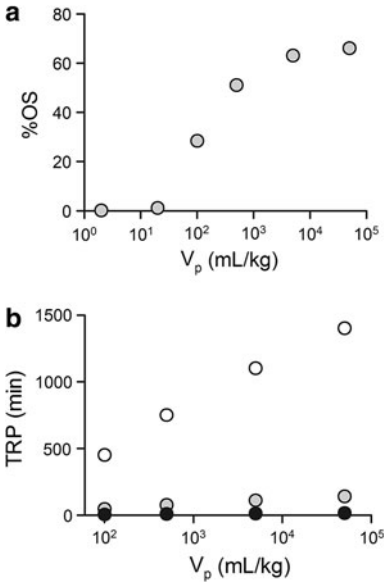

Fig. 5 Influence of clearance terms on magnitude (**a**) and duration (**b**) of overshoot in brain partitioning. Clearance terms were maintained at a 1:1:1 ratio, but increased from 0.25 (*open*) to 2.5 (*gray*) to 25 (*black*) ml/min/kg in separate sets of simulations

V_p associated with increased *TRP* (Fig. 5b). However, as clearances decreased from 2.5 to 0.25 ml/min/kg, the steepness of this relationship increased. Conversely, as clearances increased from 2.5 to 25 ml/min/kg, the *TRP* vs. V_p relationship became less steep, with consistent reductions in *TRP*. The magnitude of the rate change decreased as *TRP* approached the lower boundaries of the time required to return to plateau value for C_{brain}/C_{plasma}.

Influence of relative clearances: varying *CL*

In order to investigate the ability of changes in relative clearance values to perturb the overshoot vs. V_p relationship within $\{P\}_D$, each of the three clearance terms was manipulated independently within a given parameter space.

In the first set of simulations, substrate clearance out of the system from the central compartment, *CL*, was manipulated relative to CL_d and CL_{br}. Beginning with $\{P\}_D$ (all clearances set to 2.5 ml/min/kg), six parameter spaces were established by incorporating V_p values ranging from 2 ml/kg to 50 l/kg. The resulting C_{brain}/C_{plasma} vs. time profiles, identical to those illustrated in Fig. 3a, are presented in Fig. 6aii, for comparative purposes. The *CL* values in each of the six parameter spaces then were decreased 10-fold (to 0.25 ml/min/kg) or increased 10-fold (to 25 ml/min/kg), while the other two clearance terms were maintained unchanged. The resulting profiles for C_{brain}/C_{plasma} vs. time are illustrated in Fig. 6ai and 6aiii. For each set of C_{brain}/C_{plasma} vs. time profiles, *%OS* and *TRP* were calculated and plotted vs. V_p (Fig. 6b, c). Open, gray, and black-filled symbols indicate values calculated from the C_{brain}/C_{plasma} vs. time profiles in Fig. 6ai, aii and aiii, which were simulated from parameter spaces with *CL* values of 0.25, 2.5, and 25 ml/min/kg.

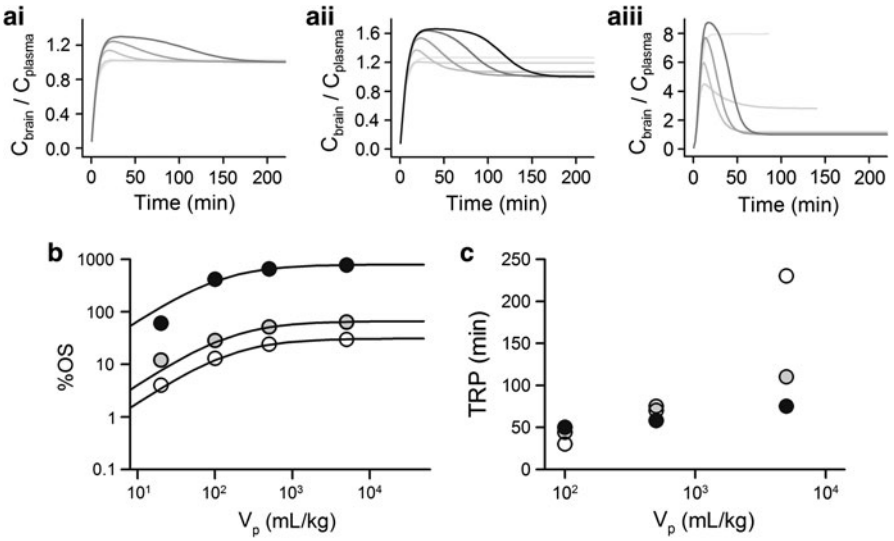

Fig. 6 Influence of systemic clearance on overshoot in brain partitioning. Simulations with $CL = 0.1$ (**ai**), 1 (**aii**), or 10 (**aiii**) times that of CL_d and CL_{br}. Profiles progressing from light to dark indicate the effect of increasing V_p from 2 ml/kg to 50 l/kg. For each scenario the resulting relationships between V_p and *%OS* and between V_p and *TRP* are illustrated (**b**, **c**). *Symbols* indicate $CL = 0.1$- (open), 1- (gray) or 10-fold (black) relative to CL_d and CL_{br}. *Lines* (**b**) indicate fit of an empirical model (Eq. 4) to the data

Table 2 Results of fitting an E_{max} model to *%OS* vs. V_p data from Figs. 6b, 7b and 8b

Relative value	0.1		1		10	
	E_{max} (%)	$V_{p,50}$ (ml\kg)	E_{max} (%)	$V_{p,50}$ (ml\kg)	E_{max} (%)	$V_{p,50}$ (ml\kg)
CL	31.0 (1.95)	159 (40.7)	66.2 (2.49)	154 (29.9)	795 (40.2)	110 (23.9)
CL_d	31.5 (1.25)	13.6 (3.82)			736 (9.96)	5220 (264)
CL_{br}	1630 (25.1)	4330 (259)			4.82 (0.0978)	29.1 (3.67)

Data are reported as parameter estimate (SE)

Relative value is the fold-difference between a clearance term and the remaining clearance terms

As *CL* increased, *%OS* values associated with a given V_p increased. The relationship between *%OS* and V_p remained consistent, with increasing V_p resulting in an increase in *%OS* up to a maximum value (Fig. 6b). An empirical model (Eq. 4) was capable of describing all three *%OS* vs. V_p profiles (the fit of the model to the data is represented by the line through each of the three relationships in Fig. 6b). Based on the model fit, the maximum *%OS* achievable by increasing V_p was 31.0, 66.2, and 795% for *CL* values of 0.25, 2.5, and 25 ml/min/kg. These values, along with the predicted volumes associated with half-maximal *%OS* values ($V_{p,50}$), are presented in Table 2.

As apparent in Fig. 6ai through iii, increasing *CL* relative to other clearance terms also changed the plateau C_{brain}/C_{plasma} values. When *CL* was relatively small

(Fig. 6ai), all hypothetical compounds reached nearly identical plateau C_{brain}/C_{plasma} values. When *CL* was relatively large (Fig. 6aiii), the plateau C_{brain}/C_{plasma} values ranged from approximately 1.3 to 7.9. The log-linear relationship between *TRP* and V_p within $\{P\}_D$ (Fig. 5b) was altered when *CL* was modulated relative to the other two clearance terms. Although the V_p-dependent increase in *TRP* was still observed, this relationship became increasingly steep as *CL* decreased relative to other clearance terms (Fig. 6c).

Influence of relative clearances: varying CL_d

A comparable set of simulations was performed to examine the impact of varying the distributional clearance between the central and peripheral compartments on the *%OS* vs. V_p relationship within $\{P\}_D$. In this second set of simulations, the same six parameter spaces, simulated by incorporating V_p values ranging from 2 ml/kg to 50 l/kg into the default parameter space, were used to generate representative profiles for C_{brain}/C_{plasma} vs. time, illustrated again for reference in Fig. 7aii. The CL_d values in each of the six parameter spaces then were decreased 10-fold or increased 10-fold relative to the other two clearance terms, which were maintained at the original $\{P\}_D$ values of 2.5 ml/min/kg. The C_{brain}/C_{plasma} vs. time profiles resulting from decreasing and increasing CL_d are illustrated in Fig. 7ai and aiii. The corresponding *%OS* and *TRP* values calculated from each group of profiles are plotted vs. V_p in Fig. 7b and c.

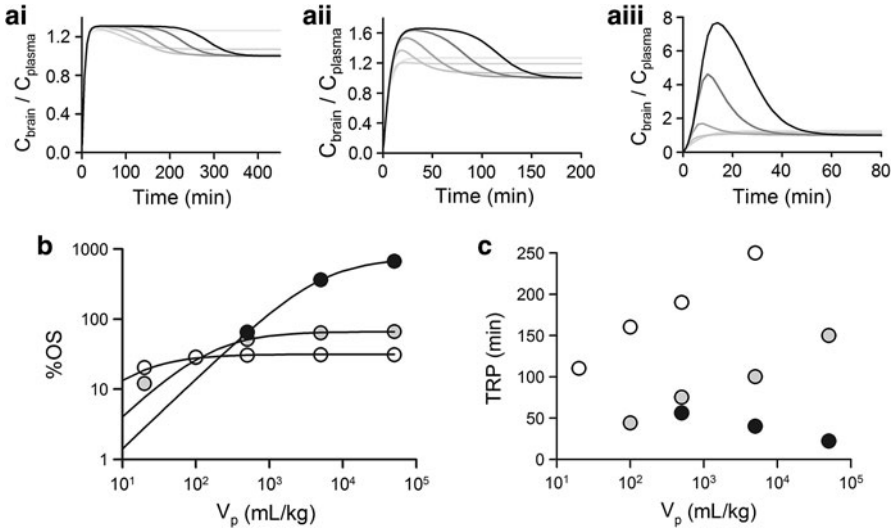

Fig. 7 Influence of CL_d on overshoot in brain partitioning. Simulations with $CL_d = 0.1$ (**ai**), 1 (**aii**), or 10 (**aiii**) times that of *CL* and CL_{br}. Profiles progressing from light to dark indicate the effect of increasing V_p from 2 ml/kg to 50 l/kg. For each scenario the resulting relationships between V_p and *%OS* and between V_p and *TRP* are illustrated (**b**, **c**). *Symbols* indicate $CL_d = 0.1$- (*open*), 1- (*gray*) or 10-fold (*black*) relative to *CL* and CL_{br}. *Lines* (**b**) indicate fit of an empirical model (Eq. 4) to the data

When V_p values were low (100 ml/kg and below), as CL_d increased the *%OS* associated with low V_p values became lower (Fig. 7b); a CL_d of 25 ml/min/kg (black symbols) ablated the overshoot observed with V_p values of 20 and 100 ml/kg. Interestingly, at high V_p values (between 0.1 and 50 l/kg) this relationship reversed, with increasingly large *%OS* values associated with increases in CL_d. These three *%OS* vs. V_p relationships also were well-fit with an empirical model (Eq. 4). The relevant parameters are presented in Table 2. Increasing the relative value of CL_d increased the maximum *%OS* predicted to be achievable by altering V_p within this parameter space. Although these E_{max} values were similar to those observed with altered *CL*, the $V_{p,50}$ values differed markedly (Table 2).

Although increasing *CL* relative to the other clearance terms resulted in increasingly different V_p-related plateau C_{brain}/C_{plasma} values (Fig. 6aiii), and decreasing the term caused all simulated systems to reach the same plateau value (Fig. 6ai), the opposite relationship was observed when manipulating CL_d (Fig. 7aiii, ai).

In all cases, increasing the relative value of CL_d reduced the *TRP* associated with changes in V_p (Fig. 7c). The positive relationship between V_p and *TRP* (apparently log-linear when CL_d was less than or equal to the other clearance terms; open and gray symbols) reversed when CL_d was relatively large (black symbols), causing a decrease in *TRP* with increasing V_p.

Influence of relative clearances: varying CL_{br}

The third set of simulations investigating relative clearance effects involved manipulation of the distributional clearance between brain and the central compartment as compared to the other two clearance processes. These simulations were conducted in a manner similar to the preceding two experiments. Figure 8ai and aiii depict the C_{brain}/C_{plasma} vs. time relationships resulting from manipulation of CL_{br} 10-fold below and 10-fold above their $\{P\}_D$ values (Fig. 8aii), within the six parameter spaces described above. The original relationship, with all clearance terms at equal values, is illustrated again for reference in Fig. 8aii. The *%OS*, and *TRP* vs. V_p relationships under each of the three relative CL_{br} conditions are illustrated in Fig. 8b and c.

The basic relationship between *%OS* and V_p was not affected by manipulating the relative value of CL_{br} (Fig. 8b). However, at a given V_p, increasing CL_{br} (black symbols) resulted in a decrease, rather than an increase, in *%OS*. The fit of an empirical model (Eq. 4) to the *%OS* vs. V_p relationships associated with the three different relative V_{br} values is illustrated with lines in Fig. 8b (parameters summarized in Table 2).

As with increasing the relative value of CL_d, increases in the relative value of CL_{br} caused the simulated C_{brain}/C_{plasma} vs. time profiles to reach nearly equal plateau values (Fig. 8aiii). *TRP* values remained virtually identical upon increasing the relative value of CL_{br} (Fig. 8c; gray and black symbols overlap). However, decreasing CL_{br} resulted in slightly shorter *TRP* when V_p was low, and substantially longer *TRP* when V_p was 5 l/kg or larger (Fig. 8c; open symbols). In all cases, increasing V_p resulted in an increased *TRP*.

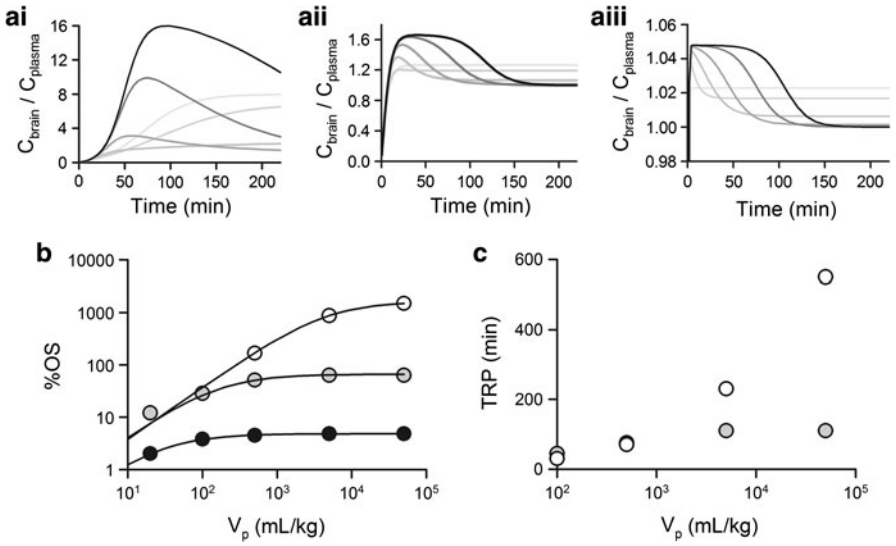

Fig. 8 Influence of CL_{br} on overshoot in brain partitioning. Simulations with $CL_{br} = 0.1$ (**ai**), 1 (**aii**), or 10 (**aiii**) times that of CL and CL_d. Profiles progressing from light to dark indicate the effect of increasing V_p from 2 ml/kg to 50 l/kg. For each scenario the resulting relationships between V_p and *%OS* and between V_p and *TRP* are illustrated (**b**, **c**). *Symbols* indicate $CL_{br} = 0.1$- (*open*), 1- (*gray*) or 10-fold (*black*) relative to CL and CL_d. *Lines* (**b**) indicate fit of an empirical model (Eq. 4) to the data

Influence of brain and plasma compartment volume

Manipulation of only the V_p term within $\{P\}_D$ allowed an indirect evaluation of the influence of the brain and plasma compartment volumes (relative to peripheral compartment volume) on the shape of the C_{brain}/C_{plasma} profile. The independent influences of the brain and plasma compartment volumes on the C_{brain}/C_{plasma} vs. time profile were assessed in the following set of simulations. As described above, based upon the fit of a sigmoidal model to the V_p vs. *%OS* relationship within $\{P\}_D$ (in which a maximum possible *%OS* of 64% could be achieved; Fig. 3b), three model parameter spaces representing low, intermediate, and high degrees of overshoot behavior ($\{P\}_1$, $\{P\}_2$ and $\{P\}_3$) were created by altering V_p within $\{P\}_D$. Beginning with these three parameter spaces, values of V_{br} or V_c were increased independently over a 50-fold range, relative to the initial values (15 and 50 ml/kg).

Figure 9a illustrates the relationship between *%OS* and V_{br} under conditions of low (open symbols), intermediate (gray symbols), and high (black symbols) degrees of V_p-related overshoot, simulated from $\{P\}_1$, $\{P\}_2$ and $\{P\}_3$. When V_p was low ($\{P\}_1$; open symbols), increasing V_{br} from the default value of 15 ml/kg to 750 ml/kg caused loss of the already minimal overshoot. When V_p was intermediate ($\{P\}_2$; gray symbols), increasing V_{br} from 15 to 30 ml/kg caused an initial increase in *%OS*; however, when V_{br} increased above 30 ml/kg, overshoot behavior decreased, then disappeared. When V_p was large ($\{P\}_3$; black symbols), such that further increases in V_p would have saturated the overshoot magnitude within $\{P\}_D$,

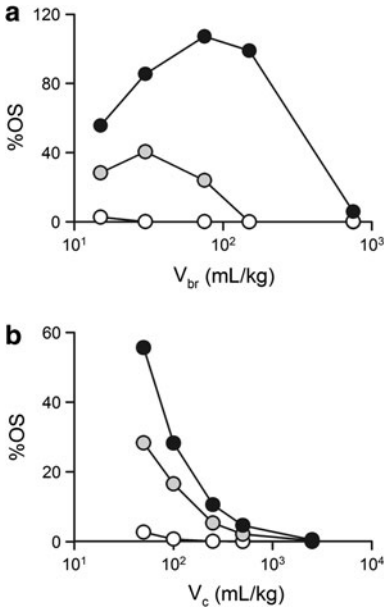

Fig. 9 Influence of V_{br} (**a**) and V_c (**b**) on overshoot in brain partitioning. Beginning with parameter spaces $\{P\}_1$ (open), $\{P\}_2$ (*gray*) or $\{P\}_3$ (*black*), V_{br} and V_c were increased separately up to 50-fold

increasing V_{br} from 15 to 75 ml/kg caused overshoot to increase up to a maximum of 107*%OS*, which was higher than the maximum *%OS* value observable by changing only V_p within $\{P\}_D$.

The relationship between overshoot and V_c, evaluated by altering the V_c value alone, was investigated beginning with the same three representative parameter spaces, $\{P\}_1$, $\{P\}_2$ and $\{P\}_3$ (Fig. 9b). In all cases, increasing V_c decreased *%OS*. The relationships between low *%OS* and low V_p (open symbols), and between high *%OS* and high V_p (black symbols) were preserved; however, when V_c was increased to 2.5 l/kg, overshoot was completely ablated, regardless of V_p.

Discussion

Principal interpretations

The present study demonstrated the influence of substrate distribution into a peripheral compartment on the tendency of the brain-to-blood partition ratio to substantially overshoot its plateau (equilibrium) value. The relationship between overshoot magnitude (*%OS*) and V_p was capacity-limited; however, the relationship between the duration of the overshoot phenomenon (*TRP*) and V_p was essentially log-linear. The relationship between either *%OS* or *TRP* and V_p was modifiable by perturbing any of the clearance terms within the system, as well as the apparent distributional volumes of the other (non-brain) system compartments. Overall, this simulation effort provides a robust framework from which to evaluate the various

system aspects that might lead to overshoot of the equilibrium value of the tissue-to-blood partition coefficient.

Although this effort was predicated on consideration of partitioning into brain, the principles developed herein are transferable to any tissue space in equilibrium with blood (i.e., for distributional processes that may be modeled with a mammillary structure), and are not dependent on the existence of a specialized barrier, such as the BBB, between that tissue space and the systemic circulation. Indeed, the simulations utilized to explore the overshoot in partitioning were based on the assumption of simple bidirectional, first-order distribution clearances. Therefore, there is no need to invoke more complex distributional processes (such as protein-mediated flux, biotransformation within the distributional compartment, or saturable protein binding in one or more compartments) between a tissue space and blood to explain overshoot in the eventual tissue-to-blood partition coefficient. In addition, overshoot in partitioning is consistent with substrate distribution in simple (linear, three-compartment) pharmacokinetic systems, although similar arguments may be made for more complex model structures (i.e., mammillary systems composed of more than three compartments). This phenomenon will be apparent when a deep peripheral pharmacokinetic compartment is present that does not contain the tissue space of interest. As long as the simulated distributional clearance rates between this organ and the systemic circulation were within the range of physiologic blood flow values, the simulation results would be applicable to any such organ.

Implications for brain partitioning behavior

The influence of peripheral compartment "depth" upon the time-dependent brain partitioning of a substrate has not, to the authors' knowledge, been commented on previously in the literature. Although not specifically stated, a general assumption, borne out by an abundance of examples, is that the tissue-to-blood partition coefficient always increases monotonically from a value of zero at the time of systemic administration to a plateau value reflecting tissue-to-blood distribution equilibrium [13]. The illustration of the effect of V_p on substrate mass in each compartment (Fig. 4) indicates that when V_p is very large, the initial rapid flux of substrate into the peripheral compartment persists longer; in addition, the larger peripheral space will retain substrate for a longer period of time (increased residence time in the peripheral compartment). The substantial diversion of substrate into the peripheral compartment initially draws substrate out of the central compartment more rapidly than out of the brain compartment, resulting in an overshoot of the plateau value for C_{brain}/C_{plasma}. As net uptake into the peripheral compartment crests and re-input of mass from this compartment begins to slowly replenish substrate in the systemic circulation (central compartment), the brain and blood compartments begin to equilibrate, resulting in the attainment of distribution equilibrium.

Relative retention of substrate within a peripheral compartment, which is required for overshoot in partitioning in an alternative compartment, may be influenced by the ratio of the distributional clearance between the peripheral and

central compartments to irreversible clearance from the central compartment. The influence of the relative values of CL and CL_d on substrate overshoot is demonstrated in Fig. 6. As CL increases relative to CL_d, the overshoot phenomenon becomes increasingly pronounced. Thus, both the apparent volume of the peripheral compartment and the distributional clearance associated with the peripheral compartment relative to systemic clearance are important determinants of substrate overshoot in the alternative (brain tissue) compartment.

In the absence of appreciation of this relatively simple kinetic explanation for overshoot and a time-dependent decrease in the brain-to-blood partition ratio, more complicated explanations for this behavior could be, and indeed have been, proposed [15, 22]. Potential alternative explanations for this type of behavior might reasonably include concentration-dependent uptake into brain from blood (e.g., saturable uptake), the existence of a capacity-limited process that clears substrate out of the brain rapidly (e.g., an efflux system at the blood–brain barrier), or saturable protein binding in blood and/or brain tissue. Experimental approaches for investigating this behavior could thus be streamlined based upon the consideration of the relationships identified by the current simulations, which is consistent with the contemporary philosophy espoused by quantitative systems pharmacology [23].

One caveat pertaining to the extrapolation of this influence of V_p on tissue partitioning kinetics is that, as noted previously [14], the appearance of this overshoot is administration mode-dependent. In a simulated system with overshoot in the C_{brain}/C_{plasma} vs. time profile, the appearance of overshoot can be abolished completely by changing the mode of input from an instantaneous bolus to a continuous constant-rate infusion. It appears, based on the above-referenced simulation study, that continuous input into the system is capable of masking the distributional kinetics between brain and blood in the presence of a "deep" peripheral compartment. This is, of course, analogous to slow absorption of substrate from the gastrointestinal tract masking substrate distribution between the systemic circulation and a peripheral space, leading to the appearance of only a single compartment after oral administration as opposed to two or more compartments after an intravenous bolus dose, as has been recognized for many years [24].

Study strengths and weaknesses

The relationship between overshoot and V_p has been demonstrated to be relatively robust within the simulated system developed here. In the present study, all system parameters were perturbed, either independently or in parallel. In most cases, the presence of overshoot was persistent over at least an order of magnitude for each parameter evaluated. The appearance of overshoot in the C_{brain}/C_{plasma} vs. time profile also was not limited to simulated systems with the same model structure; in the study described previously by the authors [14], the simulated system included an additional compartment (endothelial cells interfacing the brain and systemic compartments), as well as a unidirectional rate constant representing active efflux from endothelial cells to the central compartment. Overshoot was observed

consistently in this system when peripheral distribution volumes were large, regardless of the presence of efflux transport.

Despite the apparent reproducibility of the overshoot effect in simulated systems, several limitations of the current simulation study are acknowledged. Firstly, this study incorporated no uncontrolled error. Biologic variability, experimental assay sensitivity, and general experimental error could potentially obscure some of the relationships detected through mathematical simulations. In particular, the ability to determine the time at which a system reaches a plateau C_{brain}/C_{plasma} value would be affected by experimental error. For the purposes of this study, as no variability was present, no statistical definition of the attainment of the plateau C_{brain}/C_{plasma} value could be implemented. For this reason, the time at which the plateau C_{brain}/C_{plasma} value occurred was functionally defined as 10% of the final (plateau) C_{brain}/C_{plasma} value, although the variability in experimental measurement might reasonably exceed 10%. Nevertheless, this approach illustrates how data generated in the laboratory would need to be interpreted. Secondly, although simulated clearance rates were constrained to an upper limit below cardiac output in the rat, the range within which parameter values were manipulated in some cases spanned several orders of magnitude (i.e., representing a range of hypothetical compounds with differing pharmacokinetic behavior). Thus, the range of the parameter values simulated in these studies may not reflect conditions which would be observed commonly in in vivo pharmacokinetic systems. The evaluation of a wide range of parameter values was intended to clarify relationships which might exhibit low sensitivity in rate of change relative to another parameter of interest, rather than to mimic physiologic reality in all cases. Thirdly, the simulated system utilized in this study is substantially, although intentionally, simplistic. Protein binding in brain and plasma, physical and biochemical barriers to uptake or efflux (e.g., the BBB), metabolism, capacity-limited distribution phenomena, and other factors can influence the distribution of substrate in a physiologic system [25]. This study was intended to evaluate overshoot behavior under the simplest relevant conditions for the purposes of providing a generalized description of the fundamental behavior of the system, in the absence of any other potentially confounding factors. Based upon understanding of the behavior of this simple system, further experiments could be designed to probe the additional complexity contributed by each of these factors.

Published data supporting simulation conclusions

Although the current study, simulation-related caveats aside, has clearly and consistently demonstrated that overshoot can occur in the C_{brain}/C_{plasma} vs. time profile, it is important to recognize that this phenomenon also has been observed experimentally, with several relevant reports in the literature. For example, the antiepileptic agent valproic acid (VPA) exhibits an unusual decline in brain-to-blood partitioning with time. This pattern of time-dependent decrease in partitioning after bolus-dose administration has been observed in a variety of preclinical, in vivo experimental systems, including brain-to-blood partitioning in the cat [15], mouse [17], and rat [16, 26], and CSF-to-blood partitioning in rats [22] and in non-human primates [18]. Interestingly, VPA undergoes extensive enterohepatic recycling

(ER), wherein parent drug is conjugated in the liver, excreted into bile, and subsequently re-converted to parent drug within the intestine by intestinal β-glucuronidase and re-absorbed into the systemic circulation. This recycling loop, which retains parent compound prior to re-release into the systemic circulation, essentially functions as a large peripheral pharmacokinetic compartment [21]. A relevant issue, in the context of the current simulation study, is whether the overshoot in equilibrium brain-to-blood partitioning occurs for VPA simply because this compound recycles so extensively. A corollary question is, if recycling of VPA was ablated, would the partitioning overshoot phenomenon disappear?

As a post-hoc confirmation of the results of this simulation study, a thorough literature search on VPA brain partitioning was conducted. Examples of VPA overshoot are provided in Fig. 10 (data from [15]) and Fig. 11 (data from [22]). The ability of constant-rate infusion administration to abolish this overshoot behavior in mathematical simulations [14] also is supported by the lack of overshoot behavior in studies which utilized continuous infusion administration modes [26]. Thus, this data-mining exercise in the presence of intact VPA recycling is consistent with the current series of simulations.

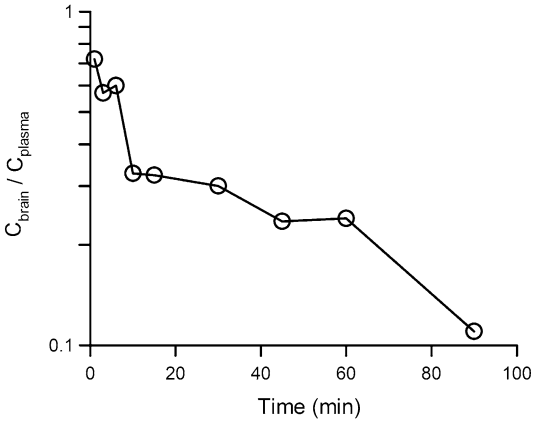

Fig. 10 The kinetics of brain-to-plasma partitioning of VPA in cats after a 3-min infusion into the inferior vena cava. Data were obtained from Hammond et al. [15]. Cerebral cortex and plasma were collected at timed intervals post-infusion, and VPA was determined by gas–liquid chromatography

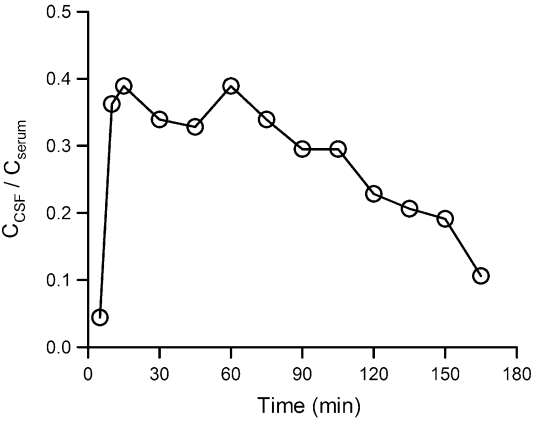

Fig. 11 The kinetics of CSF-to-serum partitioning of VPA in rats after administration by intravenous bolus plus continuous infusion. VPA was determined in CSF microdialysate. Serum concentrations were converted to estimated unbound concentrations based on separate protein binding experiments. Data were obtained from Golden et al. [22]

The relationship between overshoot in the brain-to-blood partition ratio and V_p is supported by at least two types of experimental evidence for VPA. In the current analysis of the literature data, the degree of recycling (fraction of the administered dose undergoing ER) is assumed to correspond with the apparent volume of a distributional compartment, as demonstrated previously [21]. First, a study conducted by Liu and Pollack [27] evaluated the systemic and brain disposition of VPA and two structural analogs, cyclohexanecarboxylic acid (CCA) and 1-methyl-1-cyclohexanecarboxylic acid (MCCA). These compounds differ in degree of ER as follows: VPA > MCCA ≫ CCA. The rank order of degree of ER among these compounds (Fig. 12a–c) corresponds to the degree of overshoot behavior (observed as a time-dependent decrease in C_{brain}/C_{serum}) for each compound (Fig. 12d–f). A second line of evidence pertains to the ontological development of ER capacity in the rat. Young rats, (20 days postpartum and younger), do not to exhibit intact ER (Fig. 13) [28]. The corresponding brain-to-serum partition coefficients (unpublished data; Fig. 13e–h) indicate that age-dependent appearance of ER behavior corresponds to the age-dependent appearance of overshoot in the brain partitioning profile.

While comparisons of model simulations to historical data provide an intriguing level of validation, they fall short of the mark established by prospective experimentation. VPA represents an interesting compound with which to evaluate the relationship between overshoot and V_p because there are several potential approaches to experimentally interrupt ER. These approaches include exteriorization of bile flow through bile duct cannulation [29], inhibition of β-glucuronidase activity at the level of the gut to prevent re-release of parent VPA [30], oral administration of active charcoal to decrease substrate reabsorption from the gut, and inhibition of VPA-glucuronide elimination into bile by inhibiting the activity of the canalicular efflux transporter Mrp2 [31]. These all represent potential

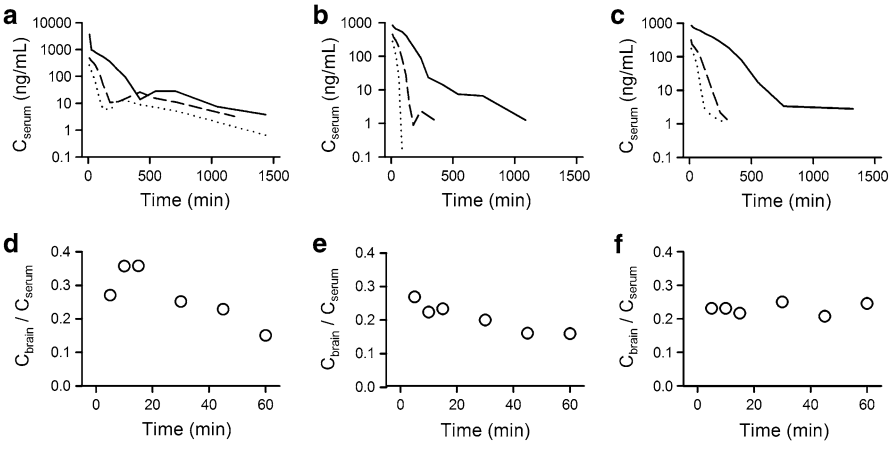

Fig. 12 Serum concentrations (**a**–**c**) and brain-to-serum concentration ratios (**d**–**f**) following i.v. bolus administration of VPA or analogs to rats. Lines (*dotted*, *dashed*, *solid*) represent doses (75, 175, or 350 mg/kg) of VPA (**a**), MCCA (**b**) and CCA (**c**). Brain-to-serum concentration ratios were determined after administration of 0.5 mmol/kg of VPA, MCCA and CCA (**d**–**f**). Data were obtained from [27]

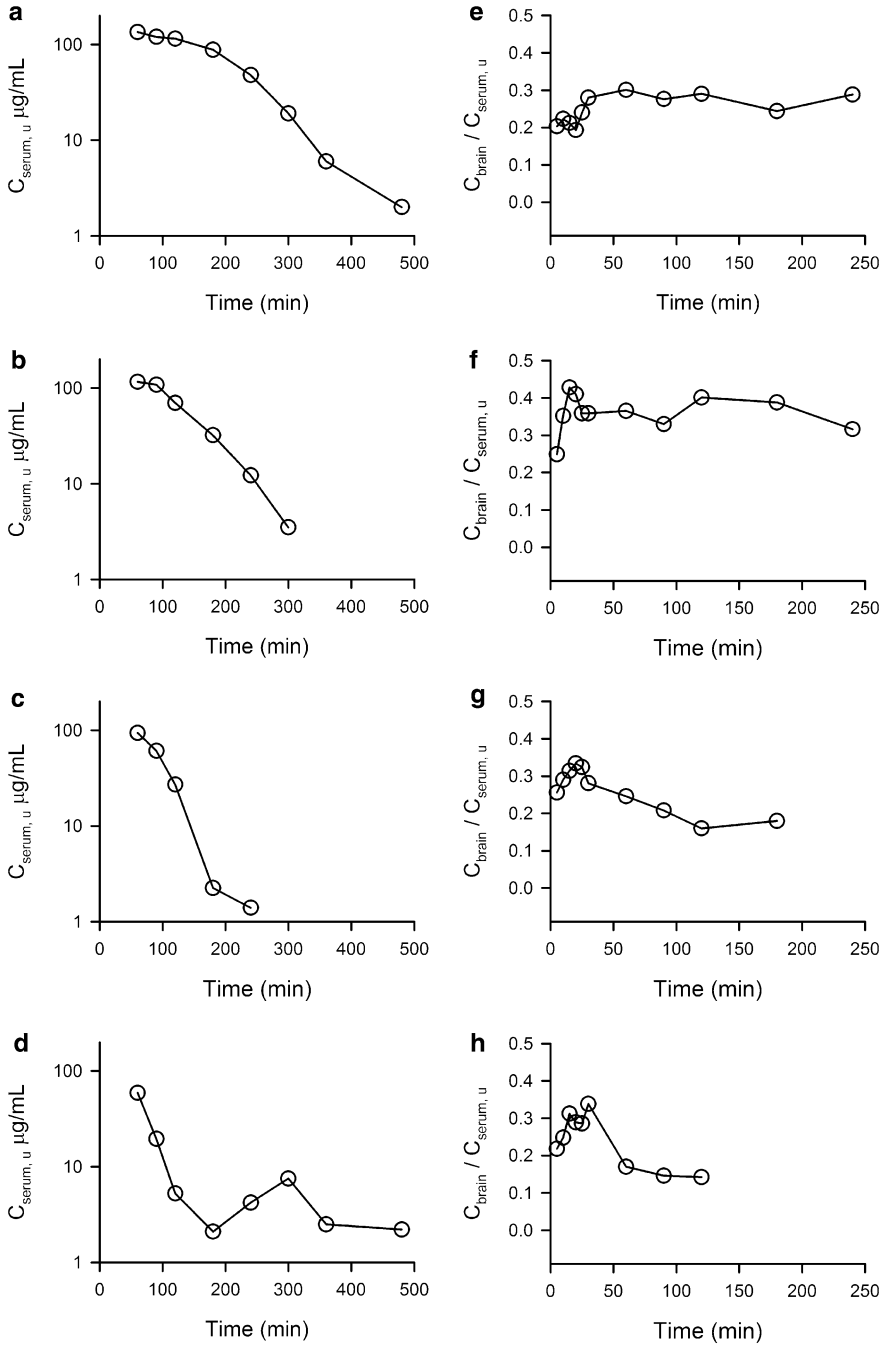

Fig. 13 Disposition of unbound VPA in serum (**a**–**d**; obtained from [28]) and brain partitioning of VPA (**e**–**h**; unpublished data) during postnatal development in rats. Ages were 5 (**a**, **e**), 10 (**b**, **f**), 20 (**c**, **g**) and 60 (**d**, **h**) days

experimental approaches to perturb the apparent volume of a distributional compartment, something that would be required for prospective evaluation of this system but extraordinarily difficult to achieve with typical distributional behavior.

Implications for accurate use of the $K_{p,brain}$ metric

The current simulation study emphasizes several caveats relevant to the use of $K_{p,brain}$ as a metric for brain exposure. Firstly, it suggests that compounds undergoing ER, or with otherwise unusually large apparent peripheral volumes of distribution (e.g., due to significant tissue binding), might be subject to the appearance of overshoot in the brain-to-blood partition coefficient vs. time profiles. Potentially, extra measures such as longer sampling time to ensure attainment of distribution equilibrium might be prudent for such compounds.

Secondly, the utility of $K_{p,brain}$ as a metric for relatively high-throughput screening of brain partitioning behavior (e.g., as a part of a pharmaceutical lead optimization strategy) is cautioned. Particularly when sampling time is limited by constraints related to the large number of samples to be processed, it is important to avoid the assumption that the peak C_{brain}/C_{plasma} value measured necessarily constitutes the true, or physiologically-relevant, $K_{p,brain}$ value. As illustrated in Fig. 7ai, when CL_d is the lowest clearance in the system the peak overshoot value persists for a relatively long time before returning to the plateau ($K_{p,brain}$) value. Misinterpretation of a persistent overshoot peak as the true $K_{p,brain}$ value may result in the erroneous pursuit of a CNS-targeted compound which only *appears* to partition significantly into the brain.

Lastly, other types of experimental observations dependent upon calculation of brain partitioning behavior could be impacted by the erroneous acceptance of an overshoot phase as a plateau value. For example, evaluation of the influence of barrier functions on brain exposure could be impacted significantly by an erroneous assumption of brain-to-blood distribution equilibrium prior to its true attainment. Compounds which exhibit efflux activity in the brain-to-blood direction reach distribution equilibrium more rapidly than in the absence of efflux [14]. Thus, evaluation of the effect of a barrier on brain exposure prior to attaining distribution equilibrium could reflect the period of time in which one system has attained distribution equilibrium, while the other would still be in flux. The net result would be an erroneous interpretation of the difference between partitioning behavior in the two systems reflecting only the effect of a barrier function at the BBB.

Conclusions

The current study demonstrates the appearance of overshoot in the brain-to-blood partition coefficient vs. time profile. This unexpected phenomenon may be interpreted, in many cases erroneously, as being indicative of complex distributional behavior. In fact, a simple pharmacokinetic system consisting of an isolated pharmacokinetic compartment (brain tissue), the systemic circulation, and a peripheral distributional compartment of relatively large apparent volume can

reproduce this behavior. Based upon the data mining exercises described above, the relationship between overshoot in tissue partitioning and V_p demonstrated in the simulated system is likely to exist in physiologic systems as well, and may explain heretofore anomalous kinetics of brain partitioning. Prospective validation studies clearly are necessary, however, to explore the degree to which these model predictions are recapitulated in vivo.

Acknowledgments This study was supported in part by the National Institutes of Health, National Institute of General Medical Sciences (Grant GM61191), Eli Lilly and Company, and NIEHS T32-ES007126.

References

1. Weaver DF, Weaver CA (2011) Exploring neurotherapeutic space: how many neurological drugs exist (or could exist)? J Pharm Pharmacol 63(1):136–139
2. Bernacki J, Dobrowolska A, Nierwinska K, Malecki A (2008) Physiology and pharmacological role of the blood-brain barrier. Pharmacol Rep 60(5):600–622
3. Neuwelt EA, Bauer B, Fahlke C, Fricker G, Iadecola C, Janigro D, Leybaert L, Molnar Z, O'Donnell ME, Povlishock JT, Saunders NR, Sharp F, Stanimirovic D, Watts RJ, Drewes LR (2011) Engaging neuroscience to advance translational research in brain barrier biology. Nat Rev Neurosci 12(3):169–182
4. Pardridge WM (2007) Drug targeting to the brain. Pharm Res 24(9):1733–1744
5. Jeffrey P, Summerfield SG (2007) Challenges for blood-brain barrier (BBB) screening. Xenobiotica 37(10–11):1135–1151
6. Patel MM, Goyal BR, Bhadada SV, Bhatt JS, Amin AF (2009) Getting into the brain: approaches to enhance brain drug delivery. CNS Drugs 23(1):35–58
7. Kalvass JC, Maurer TS, Pollack GM (2007) Use of plasma and brain unbound fractions to assess the extent of brain distribution of 34 drugs: comparison of unbound concentration ratios to in vivo p-glycoprotein efflux ratios. Drug Metab Dispos 35(4):660–666
8. Hammarlund-Udenaes M, Bredberg U, Friden M (2009) Methodologies to assess brain drug delivery in lead optimization. Curr Top Med Chem 9(2):148–162
9. Liu X, Chen C, Smith BJ (2008) Progress in brain penetration evaluation in drug discovery and development. J Pharmacol Exp Ther 325(2):349–356
10. Westerhout J, Danhof M, De Lange EC (2011) Preclinical prediction of human brain target site concentrations: considerations in extrapolating to the clinical setting. J Pharm Sci 100(9):3577–3593
11. Doran A, Obach RS, Smith BJ, Hosea NA, Becker S, Callegari E, Chen C, Chen X, Choo E, Cianfrogna J, Cox LM, Gibbs JP, Gibbs MA, Hatch H, Hop CE, Kasman IN, Laperle J, Liu J, Liu X, Logman M, Maclin D, Nedza FM, Nelson F, Olson E, Rahematpura S, Raunig D, Rogers S, Schmidt K, Spracklin DK, Szewc M, Troutman M, Tseng E, Tu M, Van Deusen JW, Venkatakrishnan K, Walens G, Wang EQ, Wong D, Yasgar AS, Zhang C (2005) The impact of P-glycoprotein on the disposition of drugs targeted for indications of the central nervous system: evaluation using the MDR1A/1B knockout mouse model. Drug Metab Dispos 33(1):165–174
12. Reichel A (2009) Addressing central nervous system (CNS) penetration in drug discovery: basics and implications of the evolving new concept. Chem Biodivers 6(11):2030–2049
13. Gibaldi M (1969) Effect of mode of administration on drug distribution in a two-compartment open system. J Pharm Sci 58(3):327–331
14. Padowski J, Pollack G (in press) Influence of time to achieve substrate distribution equilibrium between brain tissue and blood on quantitation of the blood-brain barrier P-glycoprotein effect. Brain Res
15. Hammond EJ, Perchalski RJ, Villarreal HJ, Wilder BJ (1982) In vivo uptake of valproic acid into brain. Brain Res 240(1):195–198
16. Hariton C, Ciesielski L, Simler S, Valli M, Jadot G, Gobaille S, Mesdjian E, Mandel P (1984) Distribution of sodium valproate and GABA metabolism in CNS of the rat. Biopharm Drug Dispos 5(4):409–414

17. Nau H, Loscher W (1982) Valproic acid: brain and plasma levels of the drug and its metabolites, anticonvulsant effects and gamma-aminobutyric acid (GABA) metabolism in the mouse. J Pharmacol Exp Ther 220(3):654–659
18. Stapleton SL, Thompson PA, Ou CN, Berg SL, McGuffey L, Gibson B, Blaney SM (2008) Plasma and cerebrospinal fluid pharmacokinetics of valproic acid after oral administration in non-human primates. Cancer Chemother Pharmacol 61(4):647–652
19. Dickinson RG, Harland RC, Ilias AM, Rodgers RM, Kaufman SN, Lynn RK, Gerber N (1979) Disposition of valproic acid in the rat: dose-dependent metabolism, distribution, enterohepatic recirculation and choleretic effect. J Pharmacol Exp Ther 211(3):583–595
20. Dickinson RG, Hooper WD, Eadie MJ (1984) pH-dependent rearrangement of the biosynthetic ester glucuronide of valproic acid to beta-glucuronidase-resistant forms. Drug Metab Dispos 12(2): 247–252
21. Pollack GM, Brouwer KL (1991) Physiologic and metabolic influences on enterohepatic recirculation: simulations based upon the disposition of valproic acid in the rat. J Pharmacokinet Biopharm 19(2):189–225
22. Golden PL, Brouwer KR, Pollack GM (1993) Assessment of valproic acid serum-cerebrospinal fluid transport by microdialysis. Pharm Res 10(12):1765–1771
23. Allerheiligen SR (2010) Next-generation model-based drug discovery and development: quantitative and systems pharmacology. Clin Pharmacol Ther 88(1):135–137
24. Chan KK, Gibaldi M (1985) Assessment of drug absorption after oral administration. J Pharm Sci 74(4):388–393
25. Hammarlund-Udenaes M, Paalzow LK, de Lange EC (1997) Drug equilibration across the blood-brain barrier–pharmacokinetic considerations based on the microdialysis method. Pharm Res 14(2):128–134
26. Liu MJ, Pollack GM (1994) Pharmacokinetics and pharmacodynamics of valproate analogues in rats. IV. Anticonvulsant action and neurotoxicity of octanoic acid, cyclohexanecarboxylic acid, and 1-methyl-1-cyclohexanecarboxylic acid. Epilepsia 35(1):234–243
27. Liu MJ, Pollack GM (1993) Pharmacokinetics and pharmacodynamics of valproate analogs in rats. II. Pharmacokinetics of octanoic acid, cyclohexanecarboxylic acid, and 1-methyl-1-cyclohexanecarboxylic acid. Biopharm Drug Dispos 14(4):325–339
28. Haberer LJ, Pollack GM (1994) Disposition and protein binding of valproic acid in the developing rat. Drug Metab Dispos 22(1):113–119
29. Liu MJ, Brouwer KL, Pollack GM (1992) Pharmacokinetics and pharmacodynamics of valproate analogs in rats III Pharmacokinetics of valproic acid, cyclohexanecarboxylic acid, and 1-methyl-1-cyclohexanecarboxylic acid in the bile-exteriorized rat. Drug Metab Dispos 20(6):810–815
30. Tsuji A, Terasaki T, Takabatake Y, Tenda Y, Tamai I, Yamashima T, Moritani S, Tsuruo T, Yamashita J (1992) P-glycoprotein as the drug efflux pump in primary cultured bovine brain capillary endothelial cells. Life Sci 51(18):1427–1437
31. Wright AW, Dickinson RG (2004) Abolition of valproate-derived choleresis in the Mrp2 transporter-deficient rat. J Pharmacol Exp Ther 310(2):584–588